Taylor & Francis
Taylor & Francis Group

Journal of Asian Architecture and Building Engineering

ISSN: 1346-7581 (Print) 1347-2852 (Online) Journal homepage: https://www.tandfonline.com/loi/tabe20

# Fire Behavior of Full-Scale CFRP-Strengthened RC Beams Protected with Different Insulation Systems

Kun Dong, Kexu Hu & Wanyang Gao

**To cite this article:** Kun Dong, Kexu Hu & Wanyang Gao (2016) Fire Behavior of Full-Scale CFRP-Strengthened RC Beams Protected with Different Insulation Systems, Journal of Asian Architecture and Building Engineering, 15:3, 581-588, DOI: 10.3130/jaabe.15.581

**To link to this article:** https://doi.org/10.3130/jaabe.15.581



Published online: 24 Oct 2018.

# Fire Behavior of Full-Scale CFRP-Strengthened RC Beams Protected with Different Insulation Systems

Kun Dong[1], Kexu Hu*[2] and Wanyang Gao[3]

[1] Ph.D. Candidate, Research Institute of Structural Engineering and Disaster Reduction, Tongji University, China
[2] Professor, Research Institute of Structural Engineering and Disaster Reduction, Tongji University, China
[3] Postdoctoral Fellow, Department of Civil and Environmental Engineering, Hong Kong Polytechnic University, China

**Abstract**

In this paper, a series of experimental studies conducted to investigate the fire behavior of insulated full-scale carbon-fiber-reinforced polymers (CFRP)-strengthened reinforced concrete (RC) beams is presented. Four CFRP-strengthened RC beams, respectively insulated with a thick coating system, ultrathin coating system and calcium silicate board system, were tested under ISO834 standard fire exposure. The test results revealed that satisfactory fire endurance for CFRP-strengthened concrete beams can be obtained with the protection of the three systems. The major role of fire insulation materials is to delay the failure of adhesive in the early stage and reduce the performance degradation of concrete and internal reinforced bars after the bond failure of the CFRP–concrete interface. In addition, it was indicated that effective anchorages of CFRP and reasonable anchoring constructions of the insulation system played important roles in ensuring the fire-resistant capability of CFRP-strengthened concrete beams. Further, a detailed finite element model was developed as an alternative to the standard fire test. The predicted temperature and deflection results were in good agreement with the measured ones. Based on the case studies, insulation thickness, insulation thermal conductivity, CFRP amount and load ratio were proven to be the main influences of the fire resistance of insulated CFRP-strengthened beams.

**Keywords:** RC beams; CFRP-strengthened; fire protection; fire test; numerical model

## 1. Introduction

In recent years, carbon-fiber-reinforced polymers (CFRP) have become increasingly popular in strengthening projects of concrete structures because of their vast advantages, such as high strength, low weight, endurance and convenience (Bakis *et al.* 2002; ACI 2008). However, the strength and stiffness of CFRP will be severely reduced at elevated temperatures. In particular, the bond property of the interface between CFRP and concrete will be badly deteriorated at temperatures above $T_g$, the glass transition temperature of adhesive (Mouritz and Gibson 2006; Chowdhury *et al.* 2011; Hu *et al.* 2007). Once such deteriorations have occurred, the effectiveness of the strengthening systems begins to fail, which endangers the strengthened structures. The properties of concrete and steel material will also be deteriorated at elevated temperatures (Netinger *et al.* 2011; Arioz 2007; Cooke 1988; Kankanamge and Mahendran 2011), which makes the structures more dangerous. The available research shows that it is difficult to reach a certain fire resistance rating for un-insulated CFRP-strengthened beams, whereas the same beam with fire protection can achieve significantly better fire resistance (Williams *et al.* 2008). Therefore, it is necessary and meaningful to implement fireproof protection on CFRP-strengthened concrete members, and the fire behavior of these insulated members needs more investigation.

In the last two decades, several fire tests have been conducted because of concerns regarding the performance of FRP-strengthened RC members exposed to fire. Deuring (1994) conducted fire tests on six RC beams strengthened with external CFRP strips and steel plates under ISO834 standard fire exposure. These tests showed that without fire protection, interaction between CFRP and concrete was lost in the first 10 minutes of fire exposure, whereas the insulated CFRP–concrete interfaces were able to withstand the exposure of fire for approximately 60 minutes. It was suggested that thermal insulation was quite important to maintain effective bonding under fire conditions. Blontrock *et al.* (2000) tested ten CFRP-strengthened RC beams insulated with various fire insulation schemes. Based on the test results, the authors

*Contact Author: Kexu Hu, Professor,
Research Institute of Structural Engineering and Disaster Reduction, Tongji University, 1239 Siping Road, Shanghai, China
Tel: +86-021-65986236
E-mail: kexuhu@tongji.edu.cn
*( Received October 1, 2015 ; accepted July 11, 2016 )*
DOI http://doi.org/10.3130/jaabe.15.581

concluded that mechanically anchored insulation provided more effective protection for the bond interface compared with adhesive anchored insulation. In addition, U-shaped insulation proved to be a reasonable method to improve fire endurance. Kodur *et al.* (2006) and Williams *et al.* (2006; 2008) conducted a series of tests on CFRP-strengthened RC members (column, slab and beams) protected with vermiculite-gypsum (VG) insulation and top-layer intumescent coating (EI-R) under ISO834 standard fire exposure. The results of these tests noted that 4 hours of fire endurance was attained because the internal reinforced concrete beam maintained low temperature with the protection of the insulation system, and the VG insulation can maintain the bond interface temperature below the glass transition temperature ($T_g$) for 54 min. Ahmed and Kodur (2010; 2011a) also conducted fire tests on four RC beams strengthened with CFRP and concluded that fire-induced axial restraint helps increase the load capacity of CFRP-strengthened RC beams in fire.

Chowdhury *et al.* (2008) found that CFRP-strengthened T-beams after fire tests were capable of retaining most of their original un-strengthened flexural capacity with sufficient fire protection. The tests conducted by Firmo *et al.* (2009) indicated that before the whole debonding of the strengthening system, the CFRP material acted as a "cable" fixed at the anchorage zones. These results noted that thermal insulation was urgently needed along the span, especially in the anchorage zones.

Previous research has indicated that fire protection plays a critical role in maintaining a certain fire resistance rating of CFRP-strengthened RC beams. However, most tests available in the literature express concerns about whether the fire resistance rating is reached. Few studies have been conducted to investigate the fire resistance mechanism and reasonable insulation configuration of insulated CFRP-strengthened RC beams. In this paper, both experimental and numerical studies were conducted to investigate this fire behavior.

## 2. Experimental Program

The four specimens for the fire tests, simply named L1, L2, L3 and L4, consisted of a rectangular RC beam, CFRP strengthening system and insulation system. The RC beams of specimens L1 and L2 were of 200 mm in width, 450 mm in depth and 4.7 m in span length, whereas the RC beams of specimens L3 and L4 were of 200 mm in width, 500 mm in depth and 5.2 m in span length. There were two 12 mm steel bars for L1 and L2, two 16 mm steel bars for L3 and three 20 mm steel bars for L4 as flexural reinforcement, and there were two 8 mm steel bars for L1 and L2 and two 12 mm steel bars for L3 and L4 as hanger bars. The stirrups used as shear reinforcement were of 6 mm in diameter and 200 mm in spacing.

After curing for 40 days, these RC beams were strengthened with CFRP sheets (12K-T700SC) of 200 mm in width and 0.167 mm in thickness. Two layers of CFRP sheets were then roller-applied at the beam soffit. Four pieces of U-wrap anchorages at each end were applied to provide additional anchorage. The properties of materials used in the tests are listed in Table 1., including the measured values of compressive strength *f*, nominal elastic modulus *E,* nominal thermal expansion coefficient $\alpha$ and nominal density $\rho$. In addition, the epoxy adhesive and primer (TH-PR/MER) used in tests had an elastic modulus of 2.98 GPa and a $T_g$ of 73°C after full curing.

Table 1. Structural Properties of Materials

| Material | Property | | | |
|---|---|---|---|---|
| | *f*/MPa | *E*/Mpa | $\alpha/m\cdot m^{-1}\cdot K^{-1}$ | $\rho/kg\cdot m^{-3}$ |
| Concrete | 30.7 | 30,000 | $2\times10^{-4}$ | 2400 |
| Steel Bar | 372 | 210,000 | $1.208\times10^{-5}$ | 7860 |
| CFRP | 4030 | 260,000 | $-1\times10^{-6}$ | 300 $(g\cdot m^{-2})$ |

Table 2. Thermal Properties of Insulation Materials

| Insulation Material | Property | | |
|---|---|---|---|
| | $\lambda/W\cdot K^{-1}\cdot m^{-1}$ | $c/J\cdot kg^{-1}\cdot K^{-1}$ | $\rho/kg\cdot m^{-3}$ |
| Thick Coating (SJ-2) | 0.12 | 500 | 1000 |
| Calcium Silicate Board | 0.061 | 740 | 250 |
| Ultrathin Coating (SB60-2) | 0.06 | 800 | 600 |

The strengthened beams were cured for 7 days and then applied with a U-shaped insulation system. Fig.1. shows the insulation details of the four specimens. Specimen L1 was completely protected along the entire span with a 50 mm thick fireproof coating (SJ-2) provided by Shanghai Huili Paint Company Limited. Specimen L2 was partially protected with thick fireproof coating (SJ-2) of 50 mm thickness in the anchorage zone and 20 mm thickness in the intermediate region. Layered construction of thick fireproof coating was adopted to ensure greater uniformity. On the entire length of specimen L3, a 40 mm thick calcium silicate board, produced by the Huida insulation materials Group Ltd., was glued with high-temperature adhesive. On the outside of the insulation, refractory steel wire was used for further fixation. A 1.5 mm thick ultrathin fireproof coating (SB60-2), produced by Shanghai Xinhua Fire Inhibitor Factory, was layered via roller application on specimen L4. The thermal properties of the insulation materials provided by the manufacturers are shown in Table 2.

The first series of tests on specimens L1 and L2 were conducted at the China Classification Society Shanghai Far East Fire Test Center, whereas the tests on specimens L3 and L4 were conducted at the Fire Resistance Horizontal Test Furnace at Tongji University. The test furnace consists of a fire chamber, loading device, temperature control system, and data acquisition and processing system. Eight gas burners provide thermal energy following the ISO834 fire curve while ten internal thermocouples monitor the furnace temperature during a fire test.

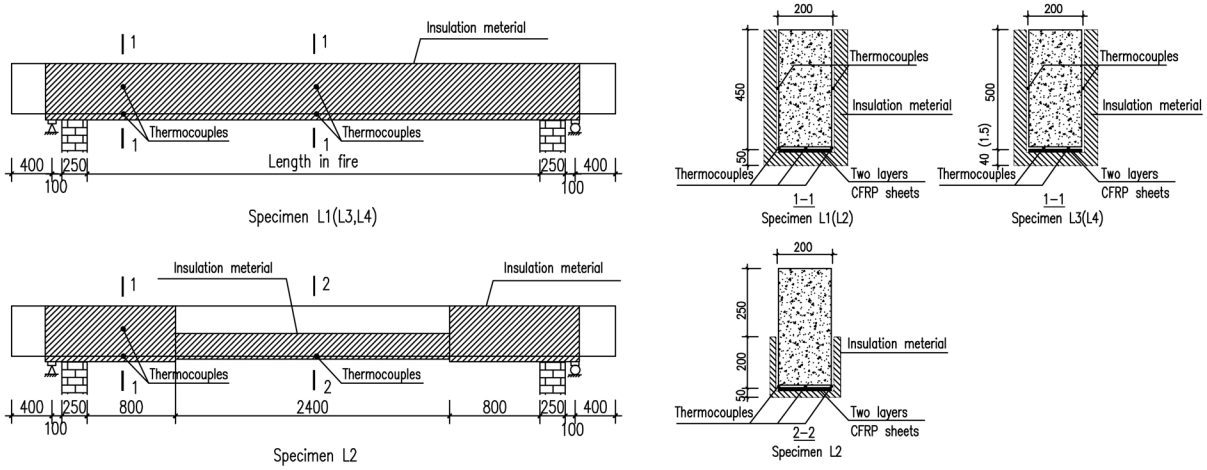


Fig.1. Insulation and Thermocouple Details for Specimens

Table 3. Details of Specimens in Fire Tests

| Specimen | Length in Fire (m) | Insulation Material | Insulation Configuration | Thickness (mm) | Anchorage Zone | Load Ratio |
|---|---|---|---|---|---|---|
| L1 | 4.0 | Thick Coating | Completely Protected | 50 | Out of Fire | 0.435 |
| L2 | 4.0 | Thick Coating | Partly Protected | 50 (20) | Out of Fire | 0.435 |
| L3 | 4.5 | Calcium Silicate Board | Completely Protected | 40 | In Fire | 0.630 |
| L4 | 4.5 | Ultrathin Coating | Completely Protected | 1.5 | In Fire | 0.630 |

As shown in Fig.1. and Table 3., the specimens were simply supported at the ends with an in-furnace length of 4.0 m for L1, L2 and 4.5 m for L3, L4. For specimens L1 and L2, the location of the CFRP anchorage zone was designed to have 250 mm in length out of the fire zone, whereas the whole strengthening zone of specimens L3 and L4 was in the fire zone. The service loads, calculated in accordance with Chinese Code GB50010, were located at 1/8, 3/8, 5/8 and 7/8 of the net span, as shown in Fig.2. The load was applied approximately 30 minutes before the start of the fire.

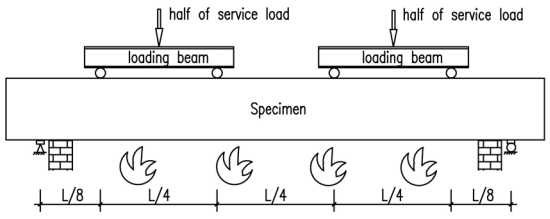


Fig.2. Loading Arrangement

The three specimen surfaces were exposed to fire and heated according to the ISO834 standard curves:

$$T - T_0 = 345\lg(8t+1)$$

where $t$ is the time of fire exposure, min; $T$ is the temperature in the furnace at moment $t$, °C; $T_0$ is the initial temperature, °C.

During the tests, Type-K thermocouples were used to measure the CFRP–concrete interface temperatures at two different sections of the specimens, as shown in Fig.1., at the bottom and side surfaces of the RC beams. In addition, mid-span deflections were measured by displacement transducers.

## 3. Test Results and Discussion

### 3.1 Thermal Response

Fig.3. shows the time–temperature progression for all specimens at the CFRP–concrete interface. It is evidently shown in Fig.3.a, Fig.3.c and Fig.3.e that the temperatures at the CFRP–concrete interfaces of specimens L1, L2 and L3, protected by thick fireproof coatings and calcium silicate board, increased slowly followed by a temperature plateau at approximately 100°C. The interface temperature at the soffit of specimen L1 reached the temperature plateau after 40 minutes of fire exposure and kept this plateau for approximately 60 minutes. For specimens L2 and L3, the temperature plateau was reached after 40 min and 60 min after the test started, and the durations on this plateau were 65 min and 20 min, respectively. This temperature plateau can be attributed to the evaporation of free and chemically bonded water in the insulation materials that consumed large amounts of energy. When the external environment was on fire, the waters in the insulation materials moved and gathered to the low temperature zone and then evaporated by absorbing heat, which reduced the temperature increase at the CFRP–concrete interface.

It should be noted that the temperature at the mid-span section of specimen L2 was significantly higher than that at the end section. This can be attributed to the falling of the insulation layers. After 27 min of fire exposure, horizontal cracks between the coating and CFRP sheets

appeared on the region where the thickness of the coating changed. After 44 min, the coating in the mid-span completely dropped to the ground, which caused the strengthened beam in the fire to have no protection. Specimen L2 then collapsed at 117 min. Referring to specimen L4, which was insulated with ultrathin fireproof intumescent coating, the temperature increase at the CFRP–concrete interface was rapid, and the temperature plateau did not appear during the test. This was due to the premature failure of the CFRP–concrete bond interface. Because the foaming temperature (100–150°C) of the ultrathin coating was higher than the glass transition temperature (73°C) of the adhesives, the bond of the interface was lost before the insulation material worked. After bond failure, debonding of CFRP sheets resulted in the ultrathin coating falling from the bottom surface. In the test on specimen L4, an interruption of ten minutes was used for obstacle checking, so a backdrop came out at approximately 95 min on the time–temperature curve.

As seen in Fig.3., the first two types of insulation materials, thick fireproof coatings and calcium silicate board, play a good insulating role in the testing process. The temperature of the interface at the side surface of specimens L1, L2 and L3 was always lower than 250°C within 120 minutes. The maximum temperatures of CFRP at the center of the bottom surface were 179°C and 198°C, respectively, for specimens L1 and L3, whereas the maximum temperature was 574°C for specimen L2 because of the early failure of insulation on the bottom surface.

It is mentioned above that the glass transition temperature $T_g$ of the adhesives used in the test was approximately 73°C. Fig.3. shows that the moment at which temperature $T_g$ was reached was after 35 min of fire exposure for specimen L1, 40 min for specimen L2, 55 min for specimen L3, and 10 min for specimen L4. These test data show that in the fire test process, although the specimens were protected with insulation materials, adhesives still failed in the early stage because of the premature achievement of temperature $T_g$. Therefore, after the bond failure of the interface, the major role of the fire insulation materials was changed to reduce the performance degradation of concrete and internal reinforced bars.

### 3.2 Structural Response

Time–deflection curves of the specimens are shown in Fig.4. The deflection progression of specimen L1 was not much different from that of specimen L2 in the early stage, which showed that partially protected

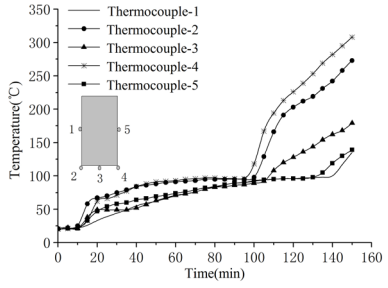


(a) Temperature at end section of L1

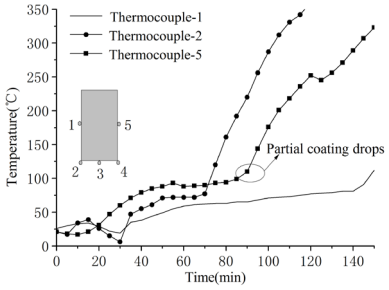


(b) Temperature at mid-span section of L1

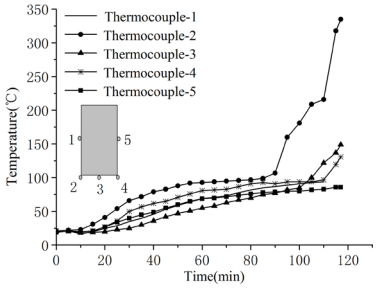


(c) Temperature at end section of L2

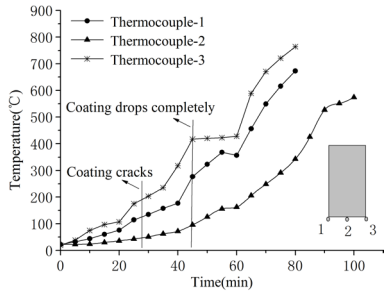


(d) Temperature at mid-span section of L2

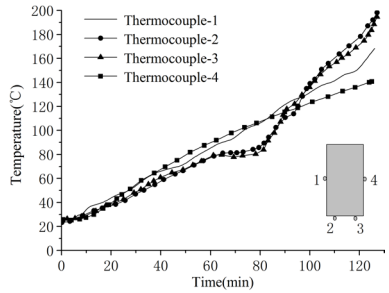


(e) Temperature at end section of L3

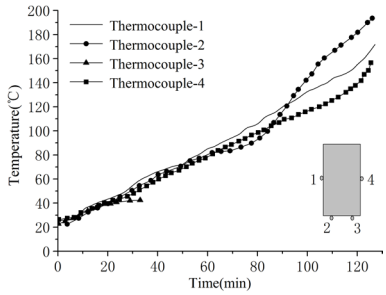


(f) Temperature at mid-span section of L3

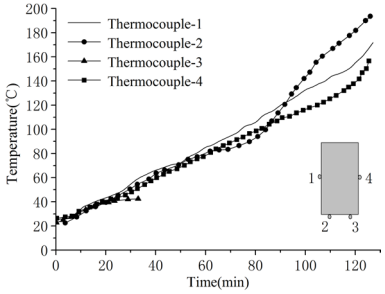


(g) Temperature at end section of L4

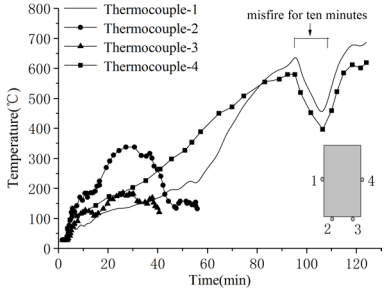


(h) Temperature at mid-span section of L4

Fig.3. Temperature Recorded at Various Locations of Beams During Fire Test

configurations worked just as well as completely protected configurations before the falling of insulation. However, when the insulation of the mid-span fell off and the CFRP sheets nearly burned out at 75 min, the CFRP-strengthened beam degenerated into the original RC beam, then the mid-span deflection of specimen L2 increased rapidly. Throughout the test, the deflection of specimen L1 increased slowly with a smaller value, which illustrated that the strengthening system of CFRP worked well with the insulation.

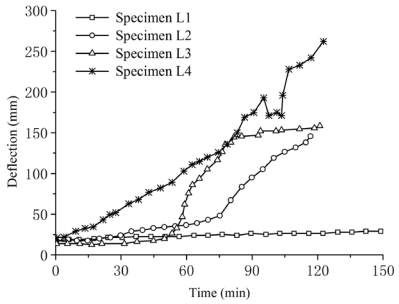


Fig.4. Time–deflection Curves of Specimens

Within 40 min after the test started, the deflection of specimen L3 was basically the same as that of specimens L1 and L2. After 50 min, the deflection of specimen L3 had a greater increase than that of specimen L1. This was due to the different positions of the CFRP anchorage zone in the tests. The anchorage zone of CFRP sheets on specimen L1 extended 250 mm outside the fire chamber, which reduced the heat-related deteriorations during the entire test. Although the bond of the interface in the mid-span was lost at high temperatures, the CFRP sheets could still work as tension reinforcement as a result of the bonding in the anchorage zone. Regarding specimen L3, the bond failure of the CFRP anchorage zone resulted in large slippage between the concrete and CFRP sheets after the temperature of adhesive exceeded $T_g$. Thenceforth, the CFRP strengthening system gradually lost effectiveness, which is why the deflection of specimen L3 increased rapidly.

Shown in Fig.4., the time–deflection curve of specimen L4 was approximately parabolic and always increased fastest. This was mainly because the strength benefit was lost after 10 min of exposure to fire. Owing to the premature failure of the CFRP strengthening system, both the service load and fire load were applied to the original RC beam. Another reason was that the load ratio for specimen L4 was higher than that for L1 and L2. Therefore, the mid-span deflection increased rapidly all the time.

## 4. Finite Element Model

As an alternative to the standard fire test, the numerical model was developed by using the ANSYS finite element analysis program (version 10.0). In the existing literature, few studies have addressed the modeling of a fire test to design fire protection systems for CFRP-strengthened RC members, including the heat transfer models (Williams 2004; Bisby *et al.* 2005; Chowdhury *et al.* 2012) and the thermal–structural model (Hawileh *et al.* 2009; Ahmed and Kodur 2011b; Dai *et al.* 2014). In this paper, an efficient 3D FE model of a CFRP-strengthened RC beam is presented to evaluate and predict its fire performance. First, three geometry models of insulated CFRP-strengthened RC beams were built. Completely protected configurations were used in these models. Second, nonlinear thermal analysis was conducted to determine the temperature distribution history of the insulated beam. After that, the nodal temperatures obtained from nonlinear thermal analysis were applied to the structural finite element model at every time point. The deflection results were then obtained in the sequentially coupled thermal–stress analysis. Both the temperature and deflection results were compared with the measured results to verify the finite element models. Finally, the effects of several insulation parameters and structural parameters on the fire behavior of an insulated CFRP-strengthened RC beam were studied with the numerical model above.

### 4.1 Thermal Analysis

In thermal analysis, the temperature distribution at a moment was related to the thermal conductivity, density and specific heat of the materials. In the fire condition, these material properties change with temperature. Based on the results suggested by Lie and Irwin (1990) and Griffic *et al.* (1981), the variations of these properties with temperature are plotted in Fig.5.(a)–5.(b). Regarding insulation materials, the thermal properties of the thick fireproof coating and ultrathin fireproof coating were assumed to be constant because of the slight change at elevated temperatures. Thermal properties of calcium silicate board were tested in the lab. Evaporation of moisture in concrete was considered with a procedure from Schaffer (1992).

There was no internally generated heat source, so the transient heat flux at the outside surfaces of the insulated strengthened beam can be regarded as a simple superposition of convection and radiation heat fluxes. To evaluate the effect of the flame convection and emissivity of the fire, the convection coefficient was assumed to be 25 W/(m$^2$·°C) for the fire-exposed surfaces and 9 W/(m$^2$·°C) for the upper surface. The resultant emissivity of the strengthened beam surface and fire was assumed to be 0.6. It should be noted that the ultrathin coating was always simulated with the average thickness after expansion, 15 mm.

The element types chosen for the transient thermal analysis are listed in Table 4., and these thermal elements will be converted to structural elements in the next structural analysis.

Table 4. The Element Types in Analysis

| Material | Analysis Type | |
|---|---|---|
| | Thermal Element | Structural Element |
| Concrete | SOLID70, 8-Node | SOLID65, 8-Node |
| Steel Bar | LINK33, 2-Node | LINK8, 2-Node |
| CFRP | SHELL57, 4-Node | SHELL41, 4-Node |
| Insulation | SOLID70, 8-Node | -- |

Fig.6.(a) and Fig.6.(b) show the comparison between the measured and the predicted temperatures at the CFRP–concrete interface. Time–temperature curves obtained from the numerical models increased almost linearly without a temperature plateau of approximately 100°C because it did not account for the evaporation and migration of free moisture in the insulation elements toward the center of the beam. However, there was still good agreement between the predicted and measured values in the early and later stages of fire exposure.

### 4.2 Thermomechanical Coupled Analysis

After the temperature distribution history of the insulated strengthened beam was determined, nonlinear thermomechanical coupled analysis was conducted sequentially. To reduce the total number of elements, both the CFRP layers and the steel bars were modelled as fully bonded to the concrete. Because little work has been conducted on the bond-slip behavior of CFRP to concrete interface at elevated temperatures, an 'effective strength model' was established to consider the deterioration of the CFRP strength and interfacial bond property. The 'effective strength model' assumed that the effective strength of externally bonded CFRP sheets at temperature $T$ could be adapted as follows:

$$f_{CE(\mathrm{T})} = \phi_{B(\mathrm{T})} \cdot \phi_{C(\mathrm{T})} \cdot f_{C0} \quad (1)$$

where $\phi_{B(\mathrm{T})}$ is the bond strength deterioration ratio of CFRP to the concrete interface at temperature $T$, $\phi_{C(\mathrm{T})}$ is the ultimate stress reduction ratio of CFRP materials at temperature $T$, and $f_{C0}$ is the strength of CFRP materials at room temperature. The deterioration ratio $\phi_{B(\mathrm{T})}$ and the reduction ratio $\phi_{C(\mathrm{T})}$, shown in Fig.5.(c), could be separately calculated by empirical models suggested by Gamage *et al.* (2005) and Bisby (2005).

The stress–strain relationships for the concrete and steel bar at elevated temperatures were adopted from Lie and Iriwn (1990). A linear elastic orthotropic constitutive relation was assumed for the FRP composites. The ultimate stress and elastic modulus of CFRP materials at different temperatures were both adopted from Bisby (2005). In addition, the bearing capacity contribution of insulation layers was neglected. The normalized variation of the strength with temperature for the constituent materials is displayed in Fig.5.(c). The element types chosen for the thermomechanical analysis are listed in Table 4.

Fig.6.(c) shows the predicted and measured mid-span vertical deflection at the centerline of the cross section as a function of fire exposure time. It is obvious that the finite element model predicted, reasonably well, the trend in the progression of the mid-span deformations with exposure time. The correlation coefficients between the predicted and measured values were 0.973 and 0.987, respectively, for temperature and mid-span deformation. The maximum difference in deformation between the FE model and the test occurred after 52 minutes of fire exposure for specimen L3, particularly because the 'effective strength model' did not fully reflect the real bond-slip behavior between CFRP and concrete interface owing to the chemical change of the matrix, especially when the interface temperature exceeded $T_g$. It must also be noted that there are several influence factors, such as shear deformation and creep, which cannot be completely considered in the FE models.

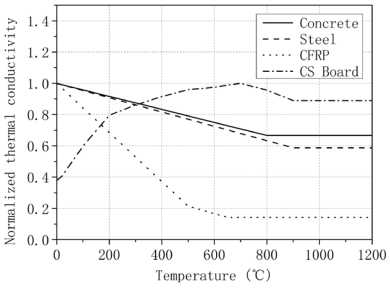


(a) Thermal conductivity

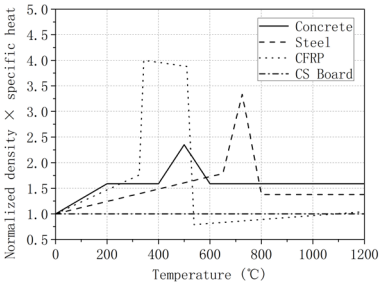


(b) Density × specific heat

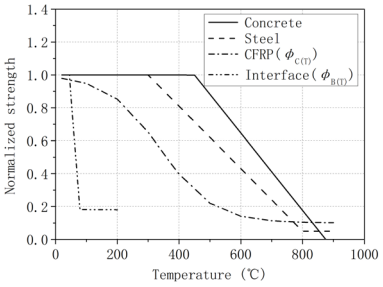


(c) Strength (yield strength for steel)

Fig.5. Normalized Thermal Properties of Materials with Elevated Temperature

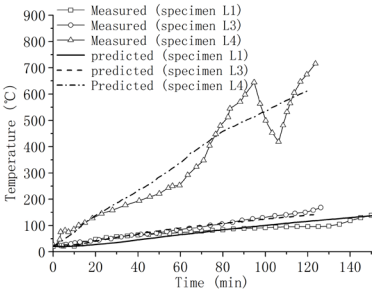


(a) Temperature at the mid-height of the beams

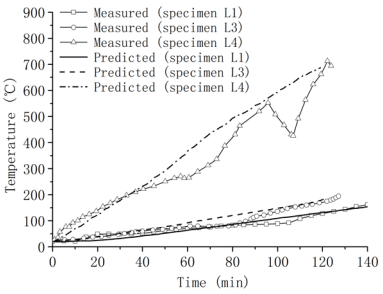


(b) Temperature at the soffit of the beams

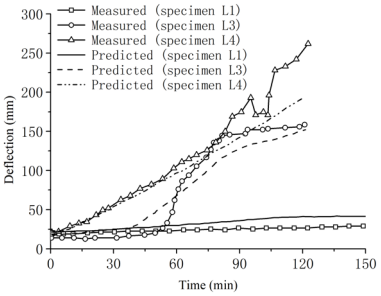


(c) Deformation at mid-span

Fig.6. Comparison between the Predicted and Measured Results at CFRP–concrete Interface

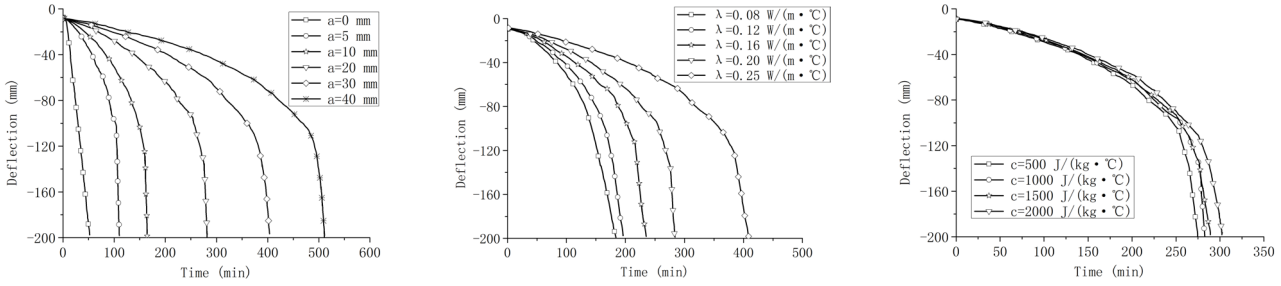


(a) Effect of insulation thickness (b) Effect of insulation thermal conductivity (c) Effect of insulation specific heat

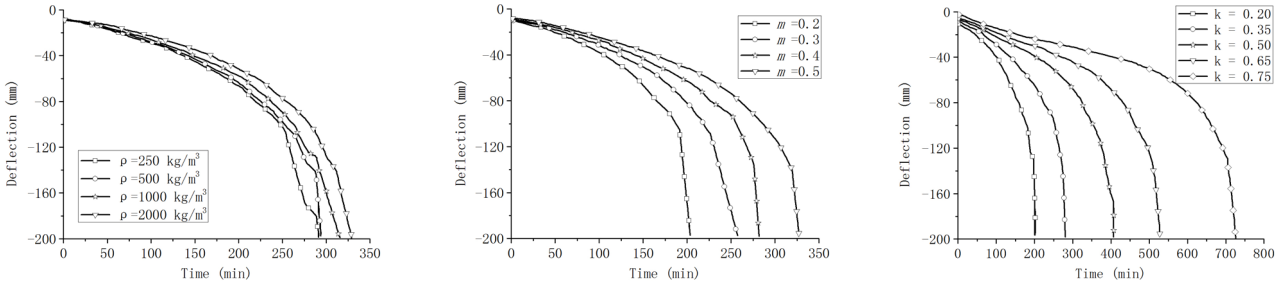


(d) Effect of insulation density (e) Effect of CFRP amounts (f) Effect of load ratio under fire

Fig.7. Deflection–time Curves Influenced by Different Parameters

### 4.3 Case Studies

To investigate the influence of the insulation parameters and structural parameters on the flexural response of the CFRP-strengthened RC beam exposed to fire, six sets of finite element models were analyzed. These parameters included insulation thickness $a$, insulation thermal conductivity $\lambda$, insulation specific heat $c$, insulation density $\rho$, CFRP amount $m$ and load ratio under fire $k$. The reference model in the case studies had dimensions of 250 mm × 400 mm × 4.0 m and the same steel reinforcement condition as specimen L4. The location of the CFRP anchorage zone was entirely on fire, thick fireproof coating and completely protected insulation configuration were used in all models, and one-twentieth of the span length (200 mm) was considered as the failure criterion. The variation ranges of parameters are listed in Table 5., where the numbers in bold belong to the reference model.

Table 5. Variation Ranges of Parameters

| Parameters | Variation Ranges |
|---|---|
| $a$ / $mm$ | 0 5 10 **20** 30 40 |
| $\lambda$ / $W{\cdot}K^{-1}{\cdot}m^{-1}$ | 0.08 **0.12** 0.16 0.20 0.25 |
| $c$ /$J{\cdot}kg^{-1}{\cdot}K^{-1}$ | 500 **1000** 1500 2000 |
| $\rho$ / $kg{\cdot}m^{-3}$ | 250 **500** 1000 2000 |
| $m$ | 0.2 **0.3** 0.4 0.5 |
| $k$ | 0.20 0.35 0.50 **0.65** 0.75 |

Deflection–time results from thermo-mechanical coupled analysis of the CFRP-strengthened RC beam, with different insulation parameters and structural parameters, are presented in Fig.7. Fig.7.(a) shows that the fire performance of a CFRP-strengthened RC beam, with a thicker insulation layer, had an obvious improvement. The deflection of the beam without insulation increased linearly and exceeded the limit value in approximately one hour, whereas the deflection of the beam with insulation thickness of 30 mm or 40 mm can reach a fire resistance of four hours. It should be mentioned that the results were slightly conservative because the cracking and delamination of the insulation layer was out of consideration. As shown in Fig.7.(b), with increasing insulation thermal conductivity, the deflection at the same moment of the insulated beam increased gradually but not linearly. Especially for the value variation from 0.08 to 0.20, the increase was significant.

It can be seen in Fig.7.(c)–7.(d) that the insulation density and specific heat had much less influence on the deflection variation. This was because different insulation densities and specific heats led to slight changes in the section temperature, not to mention the deflection caused by the degradation of material properties under high temperatures.

The CFRP amount represented the capacity increasing amplitude of the CFRP-strengthened RC beam. The load ratio under fire was defined as the ratio of the service load and the load capacity of the CFRP-strengthened RC beam. As shown in Fig.7.(e), the deflection of the insulated beam increased gradually with increasing CFRP amount when the load ratio under fire was fixed. Fig.7.(f) shows that the load ratio also had a considerable effect on the fire performance of the CFRP-strengthened RC beam, especially with the load ratio between 0.20 and 0.65. These results were mainly because the service load was almost all sustained by the original RC beam when the effectiveness of the strengthening systems failed gradually. However, after the premature failure of the CFRP strengthening system, the original RC beams still had a good fire performance owing to the existence of insulation layers.

## 5. Conclusion

Based on the experimental and numerical studies, the following conclusions can be drawn:

1. Satisfactory fire endurance of 2 hours for CFRP-strengthened concrete beams insulated with thick coating (SJ-2), calcium silicate board and ultrathin fireproof coating (SB60-2) on the whole span can be obtained. It was also indicated that U-shaped insulation for CFRP-strengthened RC beams is an effective method.

2. Although the temperature $T_g$ was reached within 60 minutes, specimens L1, L3 and L4 can continue to bear the load until the end of the test. The results showed that the major role of the insulation materials was to delay the failure of the adhesive in the early stage and reduce the performance degradation of concrete and internal reinforced bars during the later stage.

3. It can be observed from the fire test that the deflection of the specimens with the anchorage zone out of the fire was obviously smaller than that of the specimens with the anchorage zone in the fire. It was indicated that the bond effectiveness of the anchorage zone played an important role in ensuring the fire-resistant capability. If the anchorage zones of CFRP sheets were all on fire, additional anchorage measures could be applied to obtain better fire performance.

4. The predicted results agreed reasonably well with the experimental data. As a result, the models in this work were capable of predicting temperature and deflection in insulated CFRP-strengthened RC beams exposed to fire. The case studies indicated that insulation thickness, insulation thermal conductivity, CFRP amount and load ratio had significant effects on the fire resistance of insulated CFRP-strengthened RC beams, whereas the effect of insulation density and specific heat was not distinct.

## References


1) ACI Committee 440. (2008). Guide for the design and construction of externally bonded FRP systems for strengthening concrete structures. Farmington Hills, MI, USA: American Concrete Institute.
2) Arioz, O. (2007). Effects of elevated temperatures on properties of concrete. Fire Safety Journal, 42(8), pp.516-522.
3) Ahmed, A., & Kodur, V. (2010). Performance of FRP-strengthened reinforced concrete beams under design fire exposure. In Structures in Fire: Proceedings of the Sixth International Conference (p. 328). DEStech Publications, Inc.
4) Ahmed, A., & Kodur, V. (2011a). The experimental behavior of FRP-strengthened RC beams subjected to design fire exposure. Engineering Structures, 33(7), pp.2201-2211.
5) Ahmed, A., & Kodur, V. K. R. (2011b). Effect of bond degradation on fire resistance of FRP-strengthened reinforced concrete beams. Composites Part B: Engineering, 42(2), pp.226-237.
6) Bakis, C., Bank, L. C., Brown, V., Cosenza, E., Davalos, J. F., Lesko, J. J. & Triantafillou, T. C. (2002). Fiber-reinforced polymer composites for construction-state-of-the-art review. Journal of Composites for Construction, 6(2), pp.73-87.
7) Blontrock, H., Taerwe, L., & Vandevelde, P. (2000). Fire tests on concrete beams strengthened with fibre composite laminates. In Proceedings of the International PhD Symposium in Civil Engineering, Vienna (Austria), 5-7 October 2000/ed. Konrad Bergmeister. -Volume 2, pp.151-161.
8) Bisby, L. A., Green, M. F., & Kodur, V. K. R. (2005). Modeling the behavior of fiber reinforced polymer-confined concrete columns exposed to fire. Journal of Composites for Construction. 9(1), pp.15-24.
9) Chowdhury, E. U., Bisby, L. A., Green, M. F., & Kodur, V. K. (2008). Residual behavior of fire-exposed reinforced concrete beams prestrengthened in flexure with fiber-reinforced polymer sheets. Journal of Composites for Construction. 12 (1), pp.61-68.
10) Chowdhury, E. U., Eedson, R., Bisby, L. A., Green, M., & Bénichou, N. (2011). Mechanical Characterization of FRP Materials at High Temperature. Fire Technology, 47(4): 063-1080.
11) Chowdhury, E., Bisby, L., Green, M., Bénichou, N., & Kodur, V. (2012). Heat transfer and structural response modelling of FRP confined rectangular concrete columns in fire. Construction and Building Materials, 32, pp.77-89.
12) Cooke G M E. (1988). An introduction to the mechanical properties of structural steel at elevated temperatures. Fire Safety Journal, 13(1), pp.45-54.
13) Dai, J. G., Gao, W. Y., & Teng, J. G. (2014). Finite element modeling of insulated FRP-strengthened RC beams exposed to fire. Journal of Composites for Construction, 19(2), 04014046.
14) Deuring, M. (1994). Fire tests on strengthened reinforced concrete beams. Research Rep. No. 148'795, Swiss Federal Laboratories for Materials Testing and Research, Dubendorf, Switzerland.
15) Firmo, J. P., Correia, J. R., & França, P. (2012). Fire behavior of reinforced concrete beams strengthened with CFRP laminates: Protection systems with insulation of the anchorage zones. Composites: Part B, Vol. 43, No. 3, pp.1545-1556.
16) Gamage, J. C. P. H., Wong, M. B., & Al-Mahaidi, R. (2005). Performance of CFRP strengthened concrete members under elevated temperatures. In Proceedings of the international symposium on bond behavior of FRP in structures, pp.7-9.
17) Griffis, C. A., Masumura, R. A., & Chang, C. I. (1981). Thermal response of graphite epoxy composite subjected to rapid heating. Journal of Composite Materials, 15(5), pp.427-442.
18) Hawileh, R. A., Naser, M., Zaidan, W., & Rasheed, H. A. (2009). Modeling of insulated CFRP-strengthened reinforced concrete T-beam exposed to fire. Engineering Structures,31(12), pp.3072-3079.
19) Hu, K., He, G., & Lu, F. (2007). Experimental study on fire protection methods of reinforced concrete beams strengthened with carbon fiber reinforced polymer. Frontiers of Architecture and Civil Engineering in China, 1(4), pp.399-404.
20) Kankanamge N D, Mahendran M. (2011). Mechanical properties of cold-formed steels at elevated temperatures. Thin-Walled Structures, 49(49), pp.26-44.
21) Kodur, V. K. R., Bisby, L. A., & Green, M. F. (2006). Experimental evaluation of the fire behaviour of insulated FRP-strengthened reinforced concrete columns. Fire Safety Journal, 41(7), pp.547-557.
22) Lie, T. T., & Irwin, R. J. (1990). Evaluation of the fire resistance of reinforced concrete columns with rectangular cross-sections. Canada: NRC Publications Archive.
23) Mouritz, A. P., & Gibson, A. G. (2007). Fire properties of polymer composite materials. Springer Science & Business Media.
24) Netinger, I., Kesegic, I., & Guljas, I. (2011). The effect of high temperatures on the mechanical properties of concrete made with different types of aggregates. Fire safety journal, 46(7), pp.425-430.
25) Schaffer, E. L. (1992). Structural fire protection. New York: American Society of Civil Engineers.
26) Williams, B. (2004). Fire performance of FRP-strengthened reinforced concrete flexural members. Ph.D. thesis, Queen's University, Kingston, ON, Canada.
27) Williams, B., Bisby, L., Kodur, V., Green, M., & Chowdhury, E. (2006). Fire insulation schemes for FRP-strengthened concrete slabs. Composites Part A: Applied Science and Manufacturing, 37(8), pp.1151-1160.
28) Williams, B., Kodur, V., Green, M. F., & Bisby, L. (2008). Fire endurance of fiber-reinforced polymer strengthened concrete T-beams. ACI structural Journal, 105(1): 60-67.